JOURNAL OF MATERIALS SCIENCE 31 (1996) 3469–3474

Zirconium recovery from zircaloy shavings

A. E. BOHE, J. J. ANDRADE GAMBOA, E. M. LOPASSO*, D. M. PASQUEVICH*
*Consejo Nacional de Investigaciones Cientificas y Técnicas, CONICET and * Çomisión Nacional de Energia Atómica, Centro Atómico Bariloche, Rio Negro, Argentina*

A chlorination process for recovering Zr from zircaloy scrap has been studied. Zircaloy chlorination was possible at temperatures as low as 220 °C. The scale microstructure and its effect on the zircaloy reactivity was analysed using Thermogravimetric analysis (TGA), X-ray diffraction (XRD), energy dispersive X-ray spectroscopy (EDXS) and scanning electron microscopy (SEM) techniques. A solid–solid phase transformation took place into the oxide scale during the zircaloy chlorination. Zirconium, as $ZrCl_4(g)$, was separated from the oxide scale and chlorides of Cr and Fe. The effect of the reaction temperature was also analysed.

1. Introduction

Zircaloy-4 has a high economic value due to the requirements of the nuclear industry. The nominal composition of Zircaloy-4 is Zr: 98.4–97.8 wt %; Sn: 1.2–1.7 wt %; Cr: 0.07–0.13 wt % and Fe: 0.18–0.24 wt % [1]. Scrap, providing that it is substantially free of impurities, such as metal cuttings is easily returned to the production cycle. In contrast, scrap with high impurity contents, e.g. shavings, cannot be directly recycled. Depending on the process steps, shavings have different contamination levels, size, shape and oxide scale thickness [2]. Shavings with impurities, a variable content of oxygen and/or unknown origins must be classified and chemically treated before they can be recycled. In some cases the complexity of the treatment may be a determining factor in the economic possibility of recycling the shavings.

Heavily contaminated shavings still have significant commercial value if the Zr can be individually recovered. The zirconium used in zircaloy production is free of the natural Hf content, which is usually present to the extent of 1–3% [3]. The Hf-removal step is necessary to produce reactor-grade zirconium since Hf has a high neutron-absorption cross section. This requirement gives Zr a high economic value that makes attractive its recovery for reuse in nuclear applications.

The chlorination process is an economically and technically proven procedure to obtain refractory metals from ores [3–6]. This process has made possible the large scale production of Ti, Be, Ta and Nb. Recently, it was also proposed for recovering metals from spent catalysts [7]. The advantage of turning metals into metallic chlorides is based upon the fact that they are easily separable through distillation, sublimation or crystallization. Once separated and purified, chlorides are thermodynamically and kinetically easily reduced to metal by processes such as Kroll [8] or electrolysis [9]. Therefore we have recently proposed chlorination process for Zr recovery from the complex scrap of zircaloy [2]. We have demonstrated that different kinds of zircaloy shavings can be chlorinated at low temperatures [2]. However, to fully comprehend the chlorination process we present in this paper a deeper analysis of the formation and reactivity of the oxide scale and its effect on the chlorination of the underlying zircaloy.

2. Experimental

Non-isothermal and isothermal measurements of mass loss (ΔM) involved in chlorination of zircaloy shavings were carried out by thermogravimetric techniques. We used a high-sensitivity thermogravimetric system especially adapted to work with corrosive gases. This experimental set-up consists of an electrobalance (Model 2000, Cahn Instruments, Inc., Cerritos, CA), a gas line and a data-acquisition system [10]. Specimens of zircaloy shavings were placed in a quartz crucible in flow of either argon or an argon–chlorine mixture. Specimens (of initial mass M_i) were heated in these flowing atmospheres and mass changes were continuously measured. Initial specimens and oxide scales were observed with scanning electron microscopy (SEM 515, Philips Electronic Instruments) and analysed by energy dispersive X-ray spectroscopy (EDXS) (SEM 515, Philips Electronic Instruments). Crystalline phases of the alloy and the oxide scale were identified by X-ray powder diffraction analysis (XRD) (PW 1310/01, Philips Electronic Instruments, Inc., Mahwah, NJ). The relative amounts of the tetragonal phase were calculated from the Equation [11]:

$$\text{tetragonal phase (\%)} = \frac{I_t(1\,0\,1) \times 100}{I_m(\bar{1}\,1\,1) + I_m(1\,1\,1) + I_t(1\,0\,1)}$$

where $I_t(1\,0\,1)$ and $I_m(\bar{1}\,1\,1)$ and $I_m(1\,1\,1)$ are the diffraction intensities of (1 0 1) planes of the tetragonal

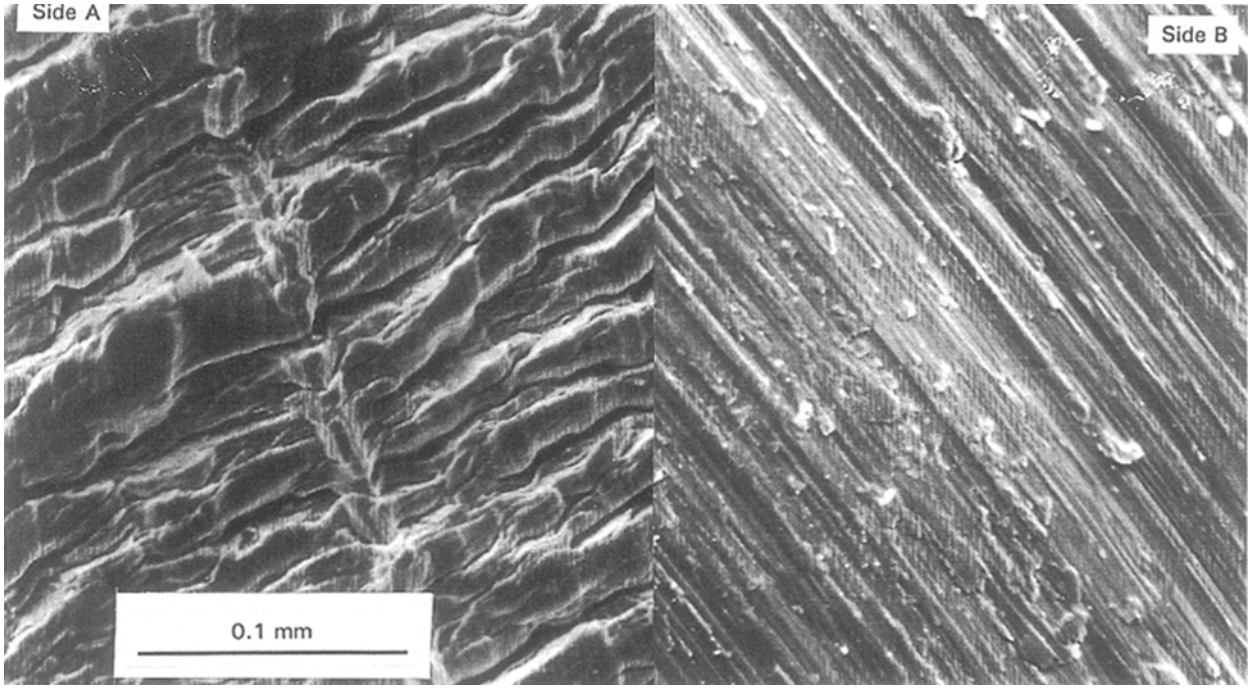

Figure 1 Sides A and B of zircaloy specimens.

phase and the ($\bar{1}$ 1 1) and (1 1 1) planes of the monoclinic phase. Shavings studied in this paper have a helical shape and a thickness lower than 0.1 mm [2]. Fig. 1 shows the appearance of the two sides of the shavings. Sides A and B have a different texture as a consequence of the mechanical treatments used in the shavings generation. The scale was formed on both sides.

3. Results and discussion

3.1. Analysis of the scale stability in a chlorine atmosphere

Fig. 2 shows the phase diagram for the zirconium–oxygen system [12] which can be applied to the understanding of the zircaloy–oxygen interaction, as has been pointed out by previous authors [13, 14]. We notice that oxygen is highly soluble in Zr. The solubility is clearly a function of temperature and the crystalline phase of the Zr. Above 862 °C Zr undergoes a phase transition. The hexagonal close-packed structure of low temperature (α-phase) transforms to the body-centred cubic structure (β-phase). Also, the zirconium dioxide has a martensitic phase transition in which the monoclinic phase transforms to a tetragonal phase above 1100 °C.

The high affinity of Zr for oxygen is the reason for the spontaneous oxidation of shavings during their formation. Oxidation of zircaloy involves not only the formation of the oxide scale on the free surface, but also the build-up of oxygen into the metal in advance of the interface, as concluded from Fig. 2. Therefore the shaving-formation temperature defines the structure of the alloy and probably its chlorine affinity. Although the shaving-formation temperature can be variable, depending on the process, it is always lower than that corresponding to the α/β transformation.

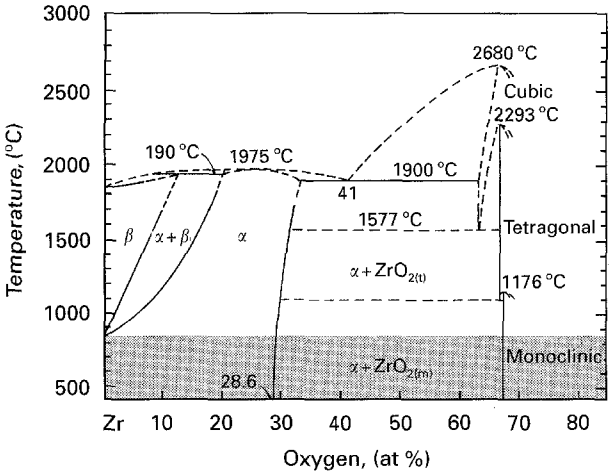

Figure 2 Phase diagram of the zirconium–oxygen system. The shaded zone represents the region in which shavings were formed.

The thermodynamically stable phases that can be observed in shavings are those contained within the shaded portion of the phase diagram illustrated in Fig. 2. Two equilibrium phases are expected: in the oxide scale, the monoclinic phase, and the α-phase, with a high oxygen content dissolved into it. The oxygen distribution at any temperature will depend upon the diffusion rate, the rate of shaving formation, the geometry of the specimen and the mechanical treatment. The last factor also affects the continuity and integrity of the oxide scale [15].

To analyse the effect of the oxide scale on the underlying alloy reactivity we have to take into account the thermodynamic stability of ZrO_2 in the presence of chlorine. Zirconium dioxide is a highly stable oxide. The reaction of chlorine with ZrO_2 is

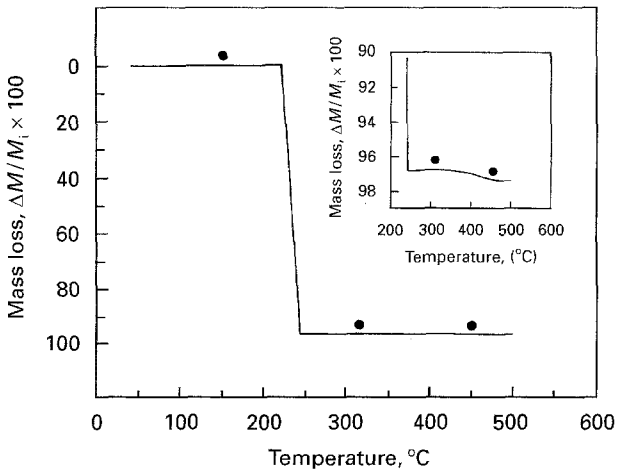

Figure 3 Effect of the chlorination temperature on zircaloy reactivity. The symbols indicate places where samples were analysed by SEM, EDXS and XRD, and the temperatures at which isothermal experiments were performed to analyse the remaining oxide phase.

represented by the following chemical equations:

$$ZrO_2(s) + 2Cl_2(g) \rightleftharpoons ZrCl_4(s) + O_2(g) \quad (1)$$

$$ZrCl_4(s) \rightleftharpoons ZrCl_4(g) \quad (2)$$

from which the standard free energy change, calculated for the overall reaction (1 + 2) is very positive. It ranges from 146–124 kJ mol^{-1} between room temperature and 1200 °C respectively [16]. The $ZrCl_4$ vapour pressure, in kPa, can be estimated from; $\log(P) = 10890 - 5400/T$, where T is the absolute temperature [17].

The thermodynamic stability of ZrO_2 should give the zircaloy a high resistance to chlorine attack. However, we can see in Fig. 3 that shaving chlorination takes place at low temperature. Fig. 3 shows a typical thermogravimetric curve obtained when zircaloy shavings were heated in a chlorine flow. The mass loss observed at about 220 °C is attributed to the beginning of the $ZrCl_4(g)$ formation since the saturated vapour pressure of $ZrCl_4$ is 0.864 kPa at this temperature. The rapid mass loss suggests that vaporization of $ZrCl_4$ takes place simultaneously with its formation and that the alloy has a high reactivity once the oxide scale was penetrated by the chlorine. The mass balance indicates a mass loss greater than 98% with respect to the initial mass. Above 400 °C we also observed an additional small mass loss, as shown in the inset-plot of Fig. 3. This additional mass loss corresponds to the chlorides volatilization, as we will discuss later.

Since the ZrO_2–Cl_2 reaction is highly unfavourable from a thermodynamic point of view, the rapid chlorination of the metal suggests that the integrity of the oxide was lowered or breached when it was heated in chlorine. Consequently, once the oxide scale was disrupted, the zircaloy rapidly reacted. The high reactivity of the alloy beneath the scale has also been recently demonstrated [2]. We have previously observed that the underlying alloy reacted with chlorine at temperatures as low as 100 °C [2]. Experiments were performed so that zircaloy chlorination was started at

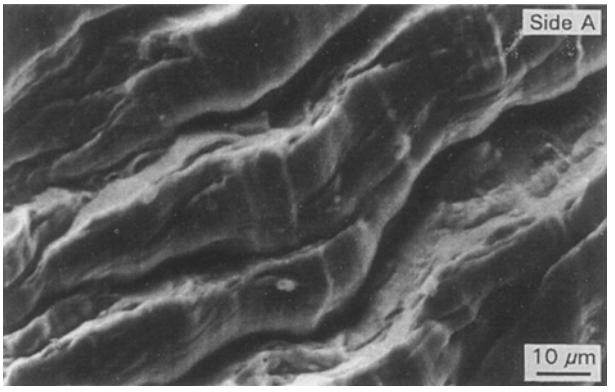

Figure 4 Surface of shavings (Side A) at chlorination temperature.

240 °C. Once the reaction progressed to about 5%, it was stopped and then the temperature was lowered in an Ar atmosphere until 100 °C. At this temperature the zircaloy was completely chlorinated as a consequence of the fact that the oxide scale, disrupted at 240 °C, was not repaired due to the absence of O_2. Thus the alloy was exposed to the chemical attack of the chlorine [2].

We analysed in detail the microstructure of the oxide scale to determine how it was disrupted. Several experiments were performed under the same conditions as those ruling the measurements plotted in Fig. 3. Symbols indicate places where chlorination was stopped and specimens were analysed. Fig. 4 shows the shaving surface before the reaction (specimen I: SI). We notice the effect of the mechanical treatment used during shaving formation. A comparison with Fig. 1 (side A) indicates that there are no appreciable modifications in the texture. Specimen I was also analysed by XRD. We verified that zircaloy was in the α-phase and that the oxide scale was very thin so that no diffraction lines of monoclinic or tetragonal zirconium oxides were observed. Once the chlorination took place we analysed the microstructure of the residues at two other temperatures, 315 °C (SII) and 450 °C (SIII). Fig. 5(a,b) show micrographs obtained for SII. We observed particles on the residue surface and cracks and flaws occurred in the scale during the chlorination, as shown in Fig. 5a. We also notice that the scale was sufficiently cracked so that volatile chlorides could easily evolve without additional damage of the scale. The large cracks were probably a consequence of an initial build up of pressure at the alloy interface due to the rapid formation of volatile chlorides. Fig. 5b shows details of deposited particles on the remaining scale. At 450 °C (see Fig. 6) the surface did not show the presence of particles. We clearly observed that the appearance of the residue surface was very similar to the surface seen in Fig. 4. Therefore the chemical attack of the scale by the chlorine was practically negligible. This observation is in agreement with the low reactivity of the ZrO_2–Cl_2 reaction indicated earlier.

The oxide scale of the original shavings was very thin so that it could not be analysed by XRD. For this reason we only observed the crystalline α-phase of the zircaloy. To determine the crystalline phase of the

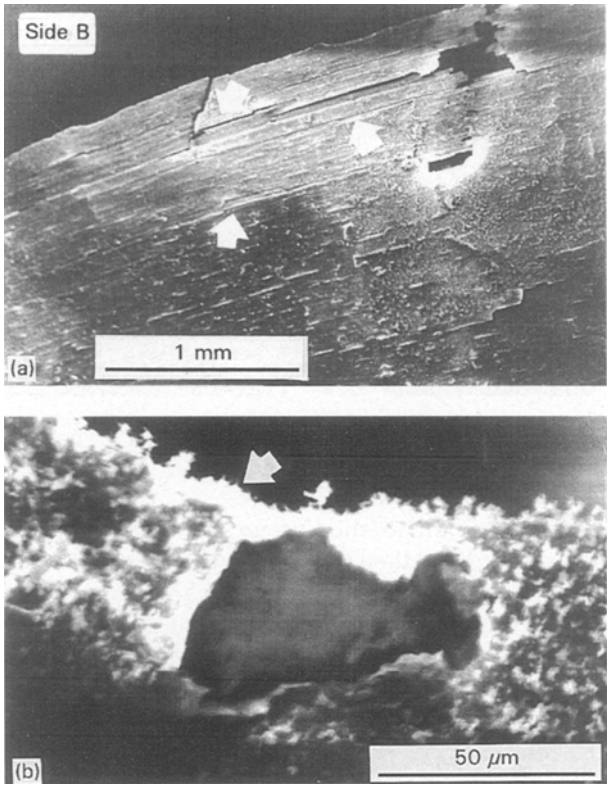

Figure 5 (a, b) Remaining solid at 315 °C. Arrows indicate cracks. Oxide scale with particles deposited on it.

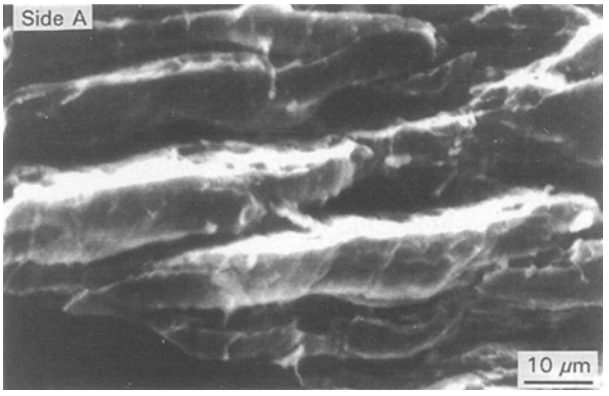

Figure 6 Remaining oxide scale.

remaining scale we performed ancillary chlorinations of large amounts of shavings. Experiments were performed at four temperatures as shown in Table I. We determined that the crystal structure of the remaining oxide was mainly the tetragonal phase, which is thermodynamically metastable at low temperatures (see Fig. 2). Since it is not possible that the tetragonal phase transformed from the monoclinic one during the chlorination we must conclude that it was originally formed with the mechanical treatment. We notice in Table I that when the chlorination temperature increased the amount of tetragonal phase decreased. Therefore, the tetragonal phase transformed to the monoclinic one during the chlorination. Since the transition phase, which is martensitic, involves an appreciable volume change (approximately 3%), we expect that the transformation of tetragonal grains

TABLE I Effect of the chlorination temperature on the relative residual mass and the crystalline phase of the oxide scale remaining.

T (°C)	(%) residue	(%) tetragonal ZrO_2 phase	(%) alpha Zr phase
20	–	ND	100
220	1.43	> 90	–
250	2.03	90	–
315	1.57	80	–
450	1.19	50	–

generates deformation in the neighbouring grains and thus stress build-up in the scale. Nonplastic materials can relax stress by means of cracks [18], as was observed in tetragonal ZrO_2 in a recent publication [19]. Stress generated during the transformation might be the primary reason for the formation of flaws or cracks through which chlorine would penetrate the scale. This possibility is in agreement with several studies on metal corrosion [20], in which oxide scale penetration by gaseous species was interpreted by means of cracks and microcracks that disrupted the oxide integrity. Moreover it was demonstrated [19] that the chlorine favours the rupture of ZrO_2 at grain boundaries, degrading cohesion and leading to intergranular separation. According with this interpretation, the penetration of the oxide scale by chlorine might start through flaws generated as a consequence of the chlorine induced tetragonal–monoclinic phase transformation. The subsequent formation of metallic chlorides would contribute to a greater degradation of the scale leading to the flaws indicated in Fig. 5a.

3.2. Effect of the temperature on the Zr separation

To determine the degree of separation of Zr from other constituents of the alloy we performed semi-quantitative EDXS analysis in different regions of specimens I to III, as indicated in Table II. Analysis of SI indicated elements composing the starting scale. The major concentration logically corresponded to Zr. In SII we performed analysis on the deposited particles and on the regions free of them. Measurements performed on the agglomerated particles showed mean concentrations of Cr, Fe and Cl greater than that on the bare surface of the scale. Analysis of SIII mainly revealed no residual Cl and very small concentrations of Cr and Fe. We attributed the particles observed in SII to metallic chlorides. We notice (Table II) that places with deposited particles had a greater concentration of chlorine, which indicated that particles would be metallic chlorides, probably of Cr and Fe.

At 315 °C the stable chlorides $CrCl_2$, $CrCl_3$, $FeCl_2$ and $FeCl_3$ were all solids whereas $SnCl_4$ was gas and $SnCl_2$ liquid [2]. These aggregation states and the low vapour pressure of the $FeCl_2$ and those of the chromium chlorides support results presented in Table II; at 315 °C tin is not observed, whereas the concentration of Cr and Fe is appreciable.

TABLE II Semiquantitative analysis (at %) by EDXS of the metals composing specimens SI, SII and SIII. The asterisks indicate analysis performed on particles deposited in SII.

Specimen	T (°C)	Zr	Cr	Sn	Fe	Cl
SI	200	98.57	0.29	0.33	3.69	–
		98.46		0.62	0.93	–
		99.53		0.47	–	–
		98.33		–	1.67	–
SII	315	62.49	8.6	–	2.03	26.88
		46.49	9.3	–	1.77	42.44
		49.58	9.68	–	1.75	38.99
		*30.32	*15.03	–	*1.37	*53.30
		46.7	15.25	–	11.71	26.34
		*16.05	*23.88	–	*5.28	*54.78
		*8.11	*28.37	–	*9.32	*54.20
SIII	450	94.8	4.19	–	0.11	–
		94.4	4.63	–	1.27	–

To understand the heating effect on the remaining scale the following equilibrium must be considered:

$$CrCl_3(s) \rightleftharpoons CrCl_2(s) + 1/2Cl_2(g) \quad (3)$$

$$CrCl_3(s) \rightleftharpoons CrCl_3(g) \quad (4)$$

$$CrCl_3(s) + 1/2Cl_2(g) \rightleftharpoons CrCl_4(g) \quad (5)$$

$$FeCl_3(s) \rightleftharpoons FeCl_3(l) \text{ (between 300 and 315 °C)} \quad (6)$$

$$2FeCl_3(l) \rightleftharpoons Fe_2Cl_6(g) \quad (7)$$

$$2FeCl_2(s) + Cl_2(g) \rightleftharpoons Fe_2Cl_6(g) \quad (8)$$

These chemical equations are written so that equilibria are shifted in favour of the reaction products when the temperature increases from 315 °C to 450 °C. The vapour pressure at the equilibrium of reaction (4) is about one order of magnitude lower than that of reaction (5) [21]. Therefore heating in a chlorine flow favours the volatilization of Cr and Fe by means of the species $CrCl_4(g)$ and $Fe_2Cl_6(g)$ respectively. The mass loss observed in the inset-plot of Fig. 3 supports the chloride volatilization. Consequently, the remaining scale shown in Fig. 6 was devoid of the chlorides previously deposited. Analysis by EDXS supported this conclusion since small amounts of Cr and Fe and none of Cl were detected in SIII (Table II).

The compositional analysis of the residues and the aggregation states of the metallic chlorides suggest that the separation of Zr from the other metals composing the alloy should be performed at about 300 °C. However, it is important to note that we have not taken into account that the oxygen content dissolved in the alpha phase might have consequences on the separation. This oxygen might lead to the formation of oxychlorides which volatilize at different temperatures. For instance, metallic iron is not volatilized in a chlorine atmosphere up to temperatures above 300 °C, but with surface adsorbed oxygen, it reacts with chlorine to form a volatile oxychloride at room temperature [22].

4. Conclusions

The results obtained in this research indicate that zircaloy chlorination is possible at low temperatures. This is a consequence of the high intrinsic reactivity of the zircaloy and little protection of the oxide scale. Breaching of the oxide may be caused by the stress generated by the tetragonal–monoclinic phase transition induced by chlorine. Chlorination of zircaloy should allow the practical separation of all the Zr as $ZrCl_4$. The residue is largely the oxide scale. The optimum temperature of chlorination to obtain a good separation appears to be 300 °C.

References

1. "Standard specification for Zirconium alloy sheet, strip, and plate for nuclear application". ASTM: B352–83.
2. A. E. BOHE, E. M. LOPASSO, J. J. ANDRADE GAMBOA and D. M. PASQUEVICH, submitted to *Mater. Sci. Tech.* (1995).
3. M. H. KLINE, in "The Metallurgy of Zirconium" (Mc Graw-Hill, New York, 1955) p. 55.
4. A. W. SCHLECHTEN, in "Rare Metals Handbook" (Reinhold, New York, 1954) p. 603.
5. C. K. GUPTA and P. K. JENA, *Trans. Indian Inst. Metals.* **336** (1965) 89.
6. J. D. GILCHRIST, in "Extraction Metallurgy" (Pergamon Press, Oxford, 1980) p. 330.
7. I. GABALLAH, M. DJONA, J. C. MUGICA and R. SOLOZOBAL, *Resources, Conservation and Recycling* **10** (1994) 87.
8. W. J. KROLL, *J. Metals* **188** (1950) 1445.
9. F. H. HAYES, H. B. BOMBERGER, F. H. FROES, L. KAUFMAN and H. M. BURTE, *ibid.* **36** (1984) 70.
10. D. M. PASQUEVICH, J. J. ANDRADE GAMBOA and A. CANEIRO, *Thermochem. Acta* **156** (1989) 275.
11. H. TORAYA, M. YOSHIMURA and S. SOMIYA, *J. Amer. Ceram. Soc.* **67** (1984) 119.
12. E. GERBHARDT, H. D. SEGHEZZI and W. DURRSCHNABEL, *J. Nucl. Mater.* **4** (1961) 255.
13. R. E. PAWEL, *ibid.* **50** (1974) 247.
14. C. J. ROSA, *J. Less-Common. Metals.* **15** (1968) 183.
15. G. L. MILLER, in "Modern Materials" (Academic Press, London, 1958) p. 308.
16. D. R. LIDE Jr, in "JANAF Thermochemical Tables, Third Edition, Part II" (American Chemical Society, Washington D.C. and American Institute of Physics, New York, 1985) p. 1691.
17. O. KUBASCHEWSKI and C. B. ALCOCK, in "Metallurgical Thermochemistry, International Series of Material Science and Technology" (Pergamon Press, Oxford, 1983) p. 376.

18. A. P. CHUPAKHIN, A. A. SAIDEL NIKOV and V. V. BOLDYREV, *React. Solids* **3** (1987) 1.
19. D. M. PASQUEVICH, F. LOVEY and A. CANEIRO, *J. Amer. Ceram. Soc.* **72** (1989) 1664.
20. F. H. STOTT, R. PRESCOTT, P. ELLIOT and M. H. J. H. AI'ATIA, *High Temp. Tech.* **6** (1988) 115.
21. K. REINHOLD and K. HAUFFE, *J. Electrochem. Soc.* **124** (1977) 875.
22. E. MURRAY, J. PRASAD, H. CABIBIL and J. A. KELBER, *Surf. Sci.* **319** (1994) 1.

Received 9 May 1995
and accepted 1 December 1995